Journal of Materials Chemistry C

Predicted Polymorph Manipulation in Exotic Double Perovskite Oxide

Journal:	*Journal of Materials Chemistry C*
Manuscript ID	TC-ART-06-2019-003367.R2
Article Type:	Paper
Date Submitted by the Author:	10-Sep-2019
Complete List of Authors:	Su, He-Ping; School of Physics, Sun Yat-Sen University Li, Shu-Fang; Key Laboratory of Bioinorganic and Synthetic Chemistry of Ministry of Education, School of Chemistry, Sun Yat-Sen University Han, Yi-Feng; Key Laboratory of Bioinorganic and Synthetic Chemistry of Ministry of Education, School of Chemistry, Sun Yat-Sen University Wu, Meixia ; School of Chemistry, Sun Yat-Sen University, Gui, Churen; School of Physics, Southeast University Chang, Yanfen; Institute of Physics Chinese Academy of Sciences Croft, Mark ; Rutgers, The State University of New Jersey Ehrlich, Steven; Brookhaven national lab., Khalid, Syed; Brookhaven national lab., Adem, Umut; Department of Materials Science and Engineering, İzmir Institute of Technolog Dong, Shuai; Southeast University, Physics Sun, Young; Institute of Physics, Chinese Academy of Sciences, Beijing National Laboratory for Condensed Matter Physics Huang, Feng; Sun Yat-sen University, Guangzhou, China, School of Physics and Engineering Li, Man-Rong; Sun Yat-Sen University, School of Chemistry ; Rutgers, The State University of New Jersey, Chemistry and Chemical Biology

ARTICLE

Predicted Polymorph Manipulation in Exotic Double Perovskite Oxide

Received 00th January 20xx,
Accepted 00th January 20xx

DOI: 10.1039/x0xx00000x

He-Ping Su,[a] Shu-Fang Li,[b,*] Yi-Feng Han,[b] Mei-Xia Wu,[b] Churen Gui,[c] Yanfen Chang,[d] Mark Croft,[e] Steven Ehrlich,[f] Syed Khalid,[f] Umut Adem,[g] Shuai Dong,[c] Young Sun,[d] Feng Huang,[h] Man-Rong Li[b,*]

Predicted polymorph manipulation offers a cutting-edge route to design function-oriented materials in exotic double perovskite-related oxide $A_2BB'O_6$ with small *A*-site cations. Herein, first-principles density functional theory calculations in light of equation of state for solid, for the first time, predict the Mg_3TeO_6 (*R*-3)-to-perovskite ($P2_1/n$) type phase transition in Mn_3TeO_6 around 5 Gpa, regardless of the deployment of magnetic interactions. High-pressure synthesis and synchrotron diffraction crystal structure analysis experimentally corroborated the polymorph variation in $Mn^{2+}{}_2Mn^{2+}Te^{6+}O_6$, which is accompanied by 13 K increasing of the antiferromagnetic ordering temperature (37 K) in the high-pressure perovskite polymorph compared to that of the ambient-pressure *R*-3 phase (24 K). The magnetodielectric coupling remains up to 50 K with maximum around the magnetic ordering temperature in the perovskite Mn_3TeO_6. The predicted polymorph manipulation here offers the possibility of accelerated materials discovery by inverse-design in exotic perovskite oxides.

Pressure-driven polymorph evolution is a pre-eminent strategy for properties-oriented materials design,[1,2] as has been extensively applied to achieve desired function in exotic perovskite-related ABO_3 and $A_2BB'O_6$ oxides with small *A*-site cations.[3-11] For examples, the multiferroic $LiNbO_3$-type (*R*3*c*) $ScFeO_3$ and $FeTiO_3$ can be achieved at 6 and 12 GPa from their ambient-pressure (AP) bixbyite (*Ia*-3) and ilmenite (*R*-3) precursors, respectively,[3, 4, 6] and the perovskite (*Pnma*) polymorph of $MnVO_3$ (a type-II multiferroics) can be synthesized from its lower-pressure (3 GPa) ilmenite analog above 5 GPa.[7] Practical magnetoelectricity has also been discovered in compounds with enhanced magnetic interactions in the transition-metal-only perovskite-related phases such as Mn_2FeMO_6 (*M* = Mo,[9] Re[10, 11]) prepared at high pressure (HP). However, so far, the pressure-dependent polymorph modification of exotic perovskites is still a high-cost and low-efficient trial-and-error process, largely due to their undistinguishable values of the geometrical descriptors like the perovskite-related tolerance factor (*t*).[12] There is not yet a universal rule to precisely govern or predict the polymorphs of a given composition. Recently, first-principles density functional theory (DFT) calculations of the total energy based on equations of state[13,14] have shed light on structure prediction of simple ABO_3 exotic perovskites, as proposed in the pressure-induced $LiSbO_3$-to-$LiNbO_3$ transition in $LiSbO_3$,[15] and ilmenite-perovskite-$LiNbO_3$ conversion in $ZnTiO_3$,[16] in which the calculated results established pressure-dependent phase stability maps of each candidate polymorph (ilmenite, perovskite, $LiNbO_3$, and $LiSbO_3$) for $LiSbO_3$ and $ZnTiO_3$ and well explained the experimentally observed phase evolution. These findings suggest possible structure prediction of exotic perovskite oxides by estimating the total energy of candidate polymorphs.

In the non-magnetic simple ABO_3-system such as $LiSbO_3$ and $ZnTiO_3$, the image is more clear than in double $A_2BB'O_6$-system, where the increased diversity of cationic arrangements yield six possible polymorphs reported to date, including distorted $GdFeO_3$-type double perovskites ($P2_1/n$), *B*-site ordered $LiSbO_3$ derivatives (*Pnn*2), Mg_3TeO_6 (*R*-3), corundum derivatives (ordered ilmenite or Ni_3TeO_6 type *R*3), bixbyite (*Ia*-3), and *β*-Li_3VF_6 (*C*2/*c*) (**Fig. 1**). Further complexity also arises from the multi-dimensional competition in magnetic $A_2BB'O_6$-system.[17] Thus, the ability to precisely predict and manipulate polymorphs requires the understanding of interplays between macroscopic (synthesis conditions) and microscopic (electronic spin, charge and orbital structures, and lattice) factors. To the best of our knowledge, so far, there is no such research work has been reported in magnetically active exotic double perovskite-related $A_2BB'O_6$ compounds to elucidate the contribution of magnetic interactions in polymorph prediction.

[a] School of Physics, Sun Yat-Sen University, Guangzhou 510275, P. R. China
[b] Key Laboratory of Bioinorganic and Synthetic Chemistry of Ministry of Education, School of Chemistry, Sun Yat-Sen University, Guangzhou 510275, P. R. China
[c] School of Physics, Southeast University, Nanjing 211189, China
[d] Beijing National Laboratory for Condensed Matter Physics, Institute of Physics, Chinese Academy of Sciences, Beijing 100190, P. R. China
[e] Department of Physics and Astronomy, Rutgers, The State University of New Jersey, Piscataway, NJ 08854, USA
[f] NSLS-II, Brookhaven National Laboratory, Upton, NY 11973, USA
[g] Department of Materials Science and Engineering, İzmir Institute of Technology, Urla 35430, İzmir, Turkey
[h] School of Materials, Sun Yat-Sen University, Guangzhou 510275, P. R. China
Email: limanrong@mail.sysu.edu.cn
Electronic Supplementary Information (ESI) available: CCDC 1912424 and 1912425. For ESI and crystallographic data in CIF or other electronic format see DOI: 10.1039/x0xx00000x

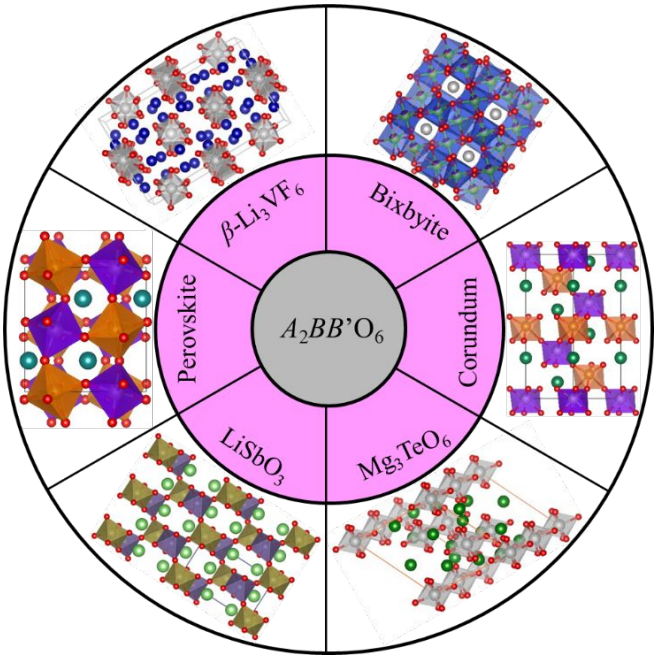

Fig. 1 Possible crystal structure types of $A_2BB'O_6$ with small *A* site cations, including distorted $GdFeO_3$-type double perovskites ($P2_1/n$), *B*-site ordered $LiSbO_3$ derivatives (*Pnn*2), Mg_3TeO_6 (*R*-3), corundum derivatives ($LiNbO_3$-type *R*3*c*, ilmenite *R*-3, and ordered ilmenite or Ni_3TeO_6 type *R*3), bixbyite (*Ia*-3), and *β*-Li_3VF_6 (*C*2/*c*).

In this work, we present for the first time the predicted polymorph manipulation in exotic double perovskite-related Mn_3TeO_6 (MTO), and study its crystal structure evolution and the accompanied physical properties variation.

AP-prepared A_3TeO_6 shows very similar *t* but adopts four possible structural types(**Fig.1**): Mg_3TeO_6-type (*R*-3) for *A* = Mg (*t* = 0.822)[18] and Mn (*t* = 0.836);[19] *β*-Li_3VF_6-type (*C*2/*c*) for *A* = Co (*t* = 0.822)[20] and Zn (*t* = 0.823);[21] polar corundum (*R*3) in Ni_3TeO_6 (*t* = 0.819);[22] and bixbyite in Cu_3TeO_6 (*t* = 0.816),[23] providing an ideal platform to understand the polymorph modification. The AP-MTO is isostructural with the rhombohedral (*R*-3) Mg_3TeO_6 as illustrated in **Figs. S1-2** and displays antiferromagnetic (AFM) type-II multiferroic behavior.[24] To investigate the structure variation of MTO under pressure, the first-principles DFT calculation in light of the equation of state for solid were conducted in three most possible polymorphs, namely *R*-3 (AP-MTO in Mg_3TeO_6), *R*3 (polar corundum Ni_3TeO_6-type), and $P2_1/n$ (distorted $GdFeO_3$-type perovskite). Chemically and geometrically, the size and charge difference between Mn^{2+} (the ionic radius in octahedral (VI) coordination ^{VI}r = 0.83 Å) and Te^{6+} (^{VI}r = 0.56 Å) energetically do not favor the formation of bixbyite *Ia*-3, $LiSbO_3$-derived *Pnn*2, or *β*-Li_3VF_6-type *C*2/*c* (Section 2.2 of Supporting Information (SI)), and thus they were not considered in the calculations. **Fig. 2** shows the variation of relative enthalpies, volume and total energy for the three types of MTO phases.[13] The enthalpy of AP-MTO is the lowest under lower-pressure conditions, while the $P2_1/n$-type structure becomes more stable at higher pressure (**Fig. 2a**). The volume of $P2_1/n$-type HP-MTO is the smallest under pressure (**Fig. 2b**). The phase transition occurring at ~ 5 GPa implies that the *R*3-type MTO is less stable than the $P2_1/n$-type HP-MTO, and hence the AP-MTO directly transforms to $P2_1/n$-type HP-MTO.

The conversion pressure of ~ 5 GPa coincides well with the experimental results, in that synthesis at 5 GPa yielded $P2_1/n$-type polymorph. Obviously, the polar *R*3 state does not appear throughout the whole calculations from the energic point of view. The quantitative results (the *ΔH* or the critical pressure shown in **Fig. 2a**) could change slightly with various calculation parameters such as the Coulomb repulsion *U* (**Table S1**), but the overall qualitative trends in the structure hold steady. Effect of Dzyaloshinskii-Moriya (DM) interaction for different proposed ferromagnetic/antiferromagnetic (FM/AFM) spin structures did not confound the overall results, therefore, in order to focus on the pressure effect on the structure, the simplest FM order was adopted in all calculations by ignoring the energy shift that complex magnetic orders may lead to.

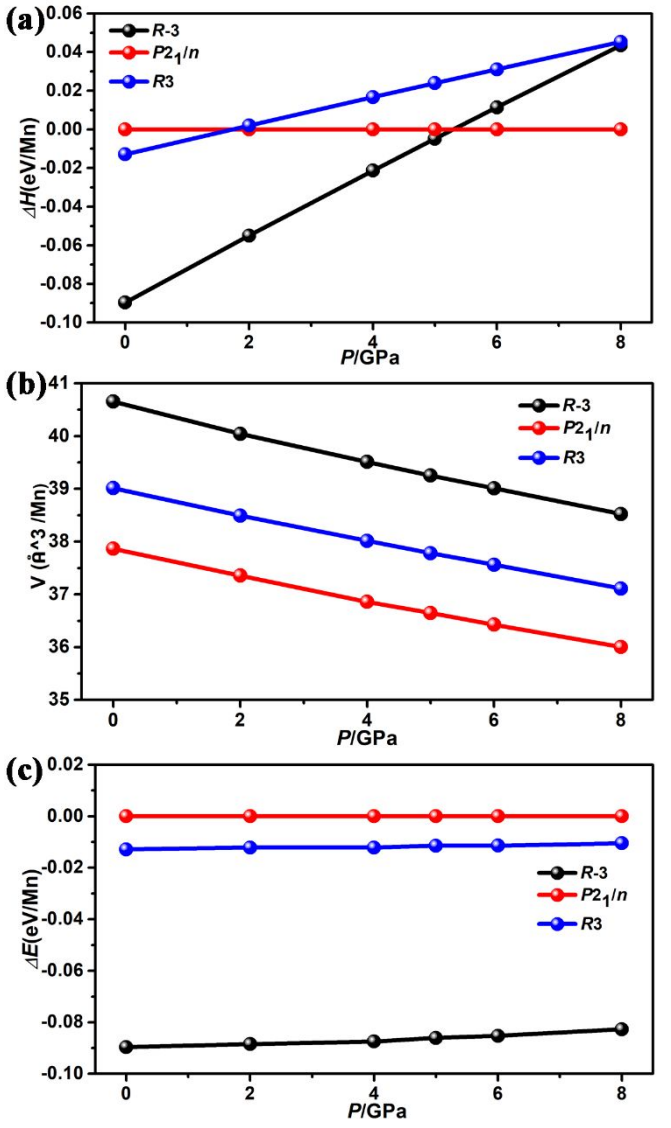

Fig. 2 Pressure dependences of the relative enthalpies (a), volume (b) and energy (c) for Mg_3TeO_6 (*R*-3), double perovskite ($P2_1/n$), and polar corundum (*R*3) types of Mn_3TeO_6.

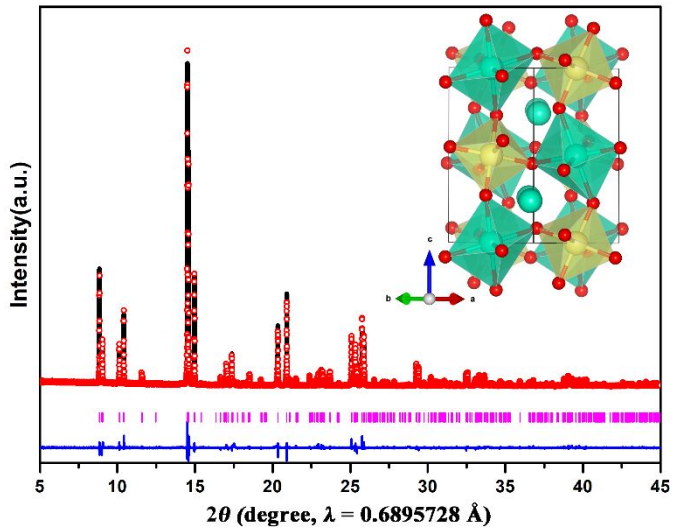

Fig. 3 Rietveld refinements from the SPXD data of HP-MTO prepared at 5 GPa and 1173 K in $GdFeO_3$-type distorted monoclinic structure ($P2_1/n$). Inset show the perspective polyhedral viewing of the unit cell structure along *c* direction. $Mn2O_6$, green; TeO_6, yellow; Mn1, green spheres; O, red spheres.

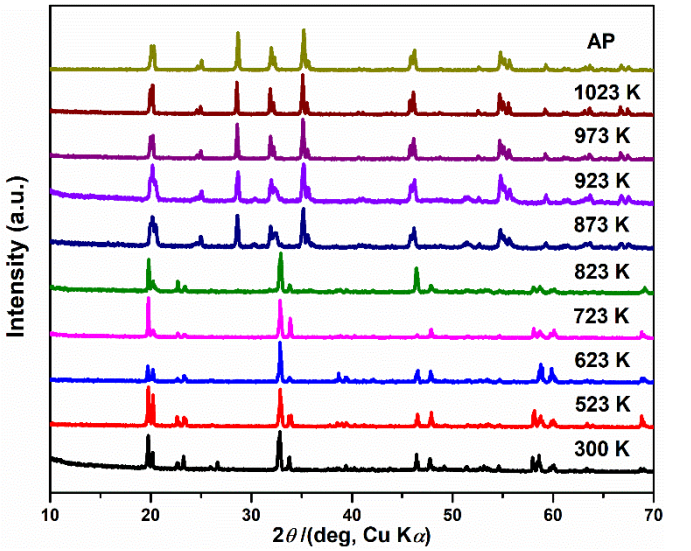

Fig. 4 Room-temperature PXD patterns of the HP-MTO after annealed between 300 and 1023 K for 30 min in Ar at each temperature point. The PXD patterns of the AP-MTO is plotted on the top for comparison. The relative intensity variation of the patterns after annealed between 300 and 873 K is owning to preferred orientation.

The HP-MTO polymorph adopts a typical monoclinic ($P2_1/n$) double perovskite structure synthesized at 5 GPa between 1173-1273 K following the prediction in **Fig. 2**, as also refined using the SPXD data in **Fig. 3**. Attempts to synthesize the HP-MTO phase below 5 GPa/1173 K were unsuccessful and yielded either the AP phase or a mixture of both polymorphs (**Fig. S3**). Dense polycrystalline pellets and small single crystals (~ 20 μm) of the HP phase can be obtained at 1173 and 1273 K, respectively, which represent identical PXD patterns. Therefore, the detailed crystal structure analyses were conducted from both powder and single crystal diffraction methods. The final refined crystallographic parameters and agreement factors are listed in **Table S2**. Selected interatomic distances, bond angles, and bond valence sums (BVS) calculations are listed in **Table S3**.

Because the crystallographic data from SPXD and single crystal diffraction approaches are almost identical within the estimated standard deviation, the results from SPXD in **Tables S2** and **S3** were used to discuss the crystal structure of HP-MTO given the higher resolution of synchrotron beamline. The crystal structure of the HP-MTO ($P2_1/n$ (No.14), a = 5.2945(1) Å, b = 5.4527(1) Å, c = 7.8092(1) Å, β = 90.37(1)°, V = 225.44 (1) Å^3, Z = 2, R_{wp} = 9.96 %, R_p = 6.50 %) is shown in the inset of **Fig. 3**, and is isostructural with other $Mn_2BB'O_6$ double perovskites.[10, 11, 25-33] The structure consists of $Mn1O_8$ coordination and rock-salt ordering of $Mn2O_6$ and TeO_6 octahedra. The average <Mn1-O> bond length (2.425(1) Å) is in line with those of the *A*-site <Mn-O> in isostructural $Mn_2BB'O_6$ varying between 2.379 and 2.406 Å,[10, 26,29,33] The <Mn2-O> of 2.175(1) Å is somewhat longer than that of the *B*-site $Mn^{2+/3+}$ (2.138(1) Å) in isostructural Mn_2MnReO_6,[28] which is reasonable considering the ionic size difference between Mn^{2+} and Mn^{3+}.[34] The TeO_6 octahedron is more regular with Te-O distance between 1.916(1) and 1.967(1) Å. Comparison of the structural parameters with the parent analogs suggests formal oxidation states of $Mn^{2+}{}_2Mn^{2+}Te^{6+}O_6$ of the HP perovskite polymorph as further corroborated by the BVS calculations (**Table S3**) and XANES analysis discussed in **Fig. S4** and Section 2.1 of SI.

The HP synthesis can enhance steric atomic interactions and induce transformation to denser structures with higher internal energy (**Fig. 2c**) related to the thermodynamic stability.[35-37] When heated at AP, a HP-phase can either decompose or revert back to the AP-phase. For example, the recently reported $LiSbO_3$-derived HP-Li_2GeTeO_6 (orthorhombic *Pnn*2, prepared at 3-5 GPa and 1073 K) can persist up to 843 K at AP before fully converting back to the AP-ordered ilmenite (*R*3) analog, accompanied by cell volume expansion with density decreasing from 5.23 to 4.97 g·cm^{-1};[37] similarly, the perovskite polymorph of Mn_2CrSbO_6 ($P2_1/n$, prepared at 8 GPa and 1473 K) undergoes a phase transition to ilmenite (*R*-3) after thermal treatment at 973 K.[27] **Fig. 4** presents the room-temperature PXD patterns of the HP-MTO (5GPa and 1273 K product) after annealing at variable temperatures. It can be seen that the $P2_1/n$ phase persisted up to 823 K, and converted back to the AP- MTO above 873 K.

The temperature dependent susceptibilities for HP-MTO measured in the field of H = 1000 Oe are shown in **Fig. 5a**. The ZFC (zero-field cooling) and FC (field cooling) curves exhibit a typically AFM behavior with Néel temperature T_N of 37 K. The Curie–Weiss (CW) temperature ϑ_{CW} from the fit to $\chi(T) = C/(T - \vartheta_{CW})$ converges to -193.98 K, indicating that the interactions in HP-MTO are AFM dominated as further evidenced by the isothermal $M(H)$ curves in **Fig. 5b**. Furthermore, the effective magnetic moment μ_{eff} of 10.23 μ_B/f. u. (formula unit) indicates S = 5/2 high-spin state of Mn^{2+} ($\mu_{eff}(Mn^{2+})$ ~ 5.89 μ_B) as evidenced by the crystal structure and XANES results. For temperatures below about 130 K, $\chi(T)$ deviates clearly from the CW behavior, suggesting that short- range correlations start to develop as manifested by slightly indicative hysteresis in **Fig. 5b**. Compared with the AP-MTO (AFM ordering below 24 K),[38] the HP-MTO orders at a higher temperature as suggested by the sharp peak at 37 K in **Fig. 5a**.

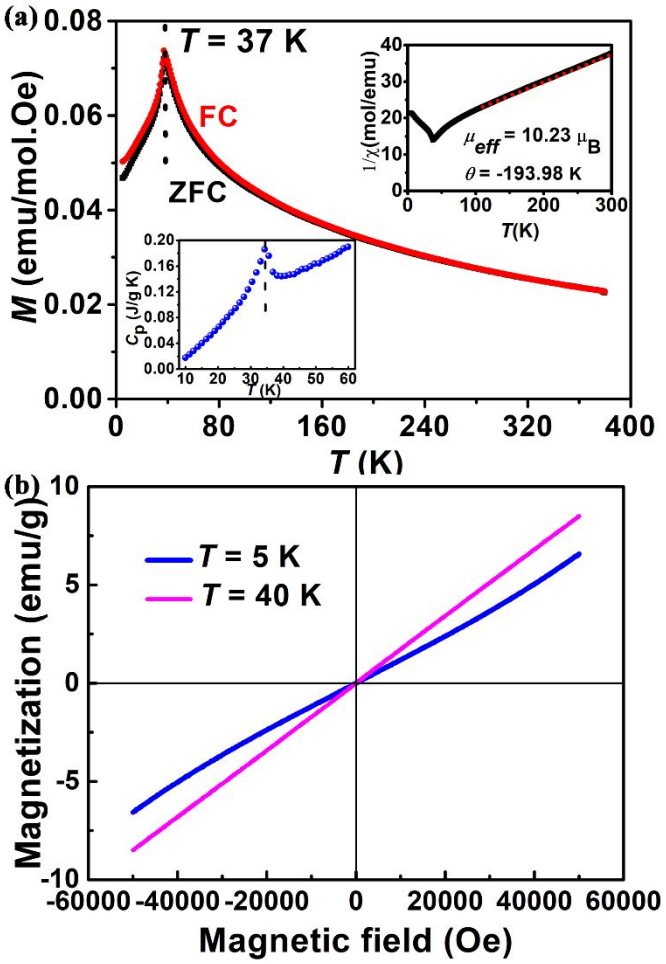

Fig. 5 (a) The temperature-dependent susceptibility and (inset) inverse susceptibility of the HP-MTO measured between 5-380 K under magnetic field of 1000 Oe. (b) Isothermal magnetization measured at 5 and 40 K, respectively.

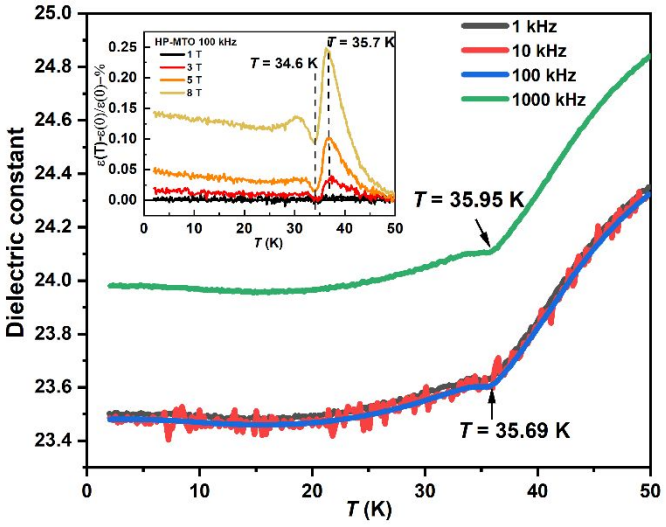

Fig. 6 Maximum magnetodielectric coupling occurs near the magnetic ordering temperature and magnetodielectric effects remain up to about 50 K.

At low temperatures, a relatively sharp peak is observed at 34.9 K in the heat capacity curve, as shown in the inset of **Fig. 5a**, which echoes the AFM transition detected in the magnetic susceptibility measurements. This latter determination of the Néel temperature is more accurate than the magnetic measurements, as closer data points were recorded in the heat capacity measurements.

Temperature dependence of the dielectric constant for the HP-MTO sample shows an anomaly at T_N = 34.6 K (**Fig. 6**), whereas no anomaly could be detected in the temperature dependence of dielectric loss. The anomaly in ε around T_N ~ 35.7 K demonstrates the presence of magnetodielectric coupling in HP-MTO. The temperature of this anomaly does shift with increasing frequency therefore dielectric relaxation effects can be ruled out. At the highest measurement frequency of 1 MHz, dielectric constant increases with respect to the measurements at lower frequencies. This kind of increase in the dielectric constant at high frequencies typically results from the inductive contribution of the measurement leads. However, this weak anomaly at T_N is not a divergent peak, suggesting the absence of ferroelectric order below T_N. There is no detectable pyroelectric response observed from the polycrystalline HP-MTO.

Apparently, the HP-MTO crystallizes in centrosymmetric space group $P2_1/n$, and unlike in the parent R-3 AP-MTO,[39] magnetic order in HP-MTO is probably not cycloidal and/or helical and does not induce ferroelectricity. Confirming the absence of ferroelectricity requires neutron diffraction experiments and further measurements on single crystal samples, which are planned as future work. Application of magnetic field slightly increases the dielectric constant and shifts the dielectric anomaly at the magnetic ordering temperature to slightly lower temperatures as shown in **Fig. 6**. Maximum magnetodielectric coupling occurs near the magnetic ordering temperature and magnetodielectric effects remain up to about 50 K.

Conclusions

In summary, the polymorph manipulation by computational prediction of the relative energetics of competing phases has been, for the first time, observed in an exotic double perovskite with small A-site cations. A pressure-induced Mg_3TeO_6 (R-3) to double perovskite ($P2_1/n$) type phase transition has been predicted to occur around 5 GPa in Mn_3TeO_6, which is further manifested by experimental synthesis and crystallographic analysis. This polymorph conversion is accompanied by about 15 K higher antiferromagnetic ordering temperature and magnetodielectric coupling in the perovskite phase. The predicted polymorph manipulation in Mn_3TeO_6 for the first time builds connection between Mg_3TeO_6 and double perovskite polymorphs, and thus broadening the platform for structure modulation in $A_2BB'O_6$. It is shown that the energetic effect of different magnetic structures could be not so critical in polymorph prediction in light of equation of state for solids, in that the energy contribution from DM interaction does not dominate the ground states of competing polymorphs. These findings will help to accelerate the discovery of new materials via data mining and high-throughput calculations in exotic $A_2BB'O_6$ (more than 13,000 new compounds by estimation under charge balance), and are of great interests for the in-

depth study of magnetic materials or access methods and properties of multifunctional materials.

Conflicts of interest

There are no conflicts to declare.

Acknowledgements

This work was financially supported by the National Science Foundation of China (NSFC-21801253, 11804404, and 21875287). Work at Brookhaven National Laboratory was supported by the DOE BES (DE-SC0012704) on the NSLS-II Beamline 7BM and on NSLS-I on the X19A. The authors thank beamline BL14B1 (Shanghai Synchrotron Radiation Facility) for providing the beam time and helps during experiments. The authors would like to thank Prof. David Walker at LDEO in Columbia University for enlightening discussions.

Notes and references

1. Y. Hamasaki, T. Shimizu, S. Yasui, T. Taniyama, O. Sakata and M. Itoh, *Cryst. Growth Des.*, 2016, **16**, 5214-5222.
2. R. Ramesh and D. G. Schlom, *Nat. Rev. Mate.*, 2019, **4**, 257-268.
3. T. Kawamoto, K. Fujita, I. Yamada, T. Matoba, S. J. Kim, P. Gao, X. Pan, S. D. Findlay, C. Tassel, H. Kageyama, A. J. Studer, J. Hester, T. Irifune, H. Akamatsu and K. Tanaka, *J. Am. Chem. Soc.*, 2014, **136**, 15291-15299.
4. M.-R. Li, U. Adem, S. R. C. McMitchell, Z. Xu, C. I. Thomas, J. E. Warren, D. V. Giap, H. Niu, X. Wan, R. G. Palgrave, F. Schiffmann, F. Cora, B. Slater, T. L. Burnett, M. G. Cain, A. M. Abakumov, G. van Tendeloo, M. F. Thomas, M. J. Rosseinsky and J. B. Claridge, *J. Am. Chem. Soc.*, 2012, **134**, 3737-3747.
5. Y. Inaguma, M. Yoshida and T. Katsumata, *J. Am. Chem. Soc.*, 2008, **130**, 6704-6705.
6. T. Varga, A. Kumar, E. Vlahos, S. Denev, M. Park, S. Hong, T. Sanehira, Y. Wang, C. Fennie, S. Streiffer, X. Ke, P. Schiffer, V. Gopalan and J. Mitchell, *Phys. Rev. Lett.*, 2009, **103**, 047601.
7. M. Markkula, A. M. Arevalo-Lopez, A. Kusmartseva, J. A. Rodgers, C. Ritter, H. Wu and J. P. Attfield, *Phys. Rev. B*, 2011, **84**, 094450.
8. J. Cong, K. Zhai, Y. Chai, D. Shang, D. D. Khalyavin, R. D. Johnson, D. P. Kozlenko, S. E. Kichanov, A. M. Abakumov, A. A. Tsirlin, L. Dubrovinsky, X. Xu, Z. Sheng, S. V. Ovsyannikov and Y. Sun, *Nat. Commun.*, 2018, **9**, 2996.
9. M.-R. Li, M. Retuerto, D. Walker, T. Sarkar, P. W. Stephens, S. Mukherjee, T. S. Dasgupta, J. P. Hodges, M. Croft, C. P. Grams, J. Hemberger, J. Sánchez-Benítez, A. Huq, F. O. Saouma, J. I. Jang and M. Greenblatt, *Angew. Chem. Int. Edit.*, 2014, **53**, 10774-10778.
10. M.-R. Li, M. Retuerto, Z. Deng, P. W. Stephens, M. Croft, Q. Huang, H. Wu, X. Deng, G. Kotliar, J. Sánchez-Benítez, J. Hadermann, D. Walker and M. Greenblatt, *Angew. Chem. Int. Edit.*, 2015, **54**, 12069-12073.
11. A. M. Arévalo-López, G. M. McNally and J. P. Attfield, *Angew. Chem. Int. Edit.*, 2015, **54**, 12074-12077.
12. M. W. Lufaso and P. M. Woodward, *Acta Crystallogr. Sec. B*, 2001, **57**, 725-738.
13. F. D. Murnaghan, *Proc. Nati. Acad. Sci.*, 1944, **30**, 244-247.
14. C. Collins, M. S. Dyer, A. Demont, P. A. Chater, M. F. Thomas, G. R. Darling, J. B. Claridge and M. J. Rosseinsky, *Chem. Sci.*, 2014, **5**, 1493-1505.
15. Y. Inaguma, A. Aimi, D. Mori, T. Katsumata, M. Ohtake, M. Nakayama and M. Yonemura, *Inorg. Chem.*, 2018, **57**, 15462-15473.
16. Y. Inaguma, A. Aimi, Y. Shirako, D. Sakurai, D. Mori, H. Kojitani, M. Akaogi and M. Nakayama, *J. Am. Chem. Soc.*, 2014, **136**, 2748-2756.
17. D. Yi, N. Lu, X. Chen, S. Shen and P. Yu, *J. Phys.: Condens. Matter*, 2017, **29**, 443004.
18. G. Blasse and W. Hordijk, *J. Solid State Chem.*, 1972, **5**, 395-397.
19. H. Singh, A. K. Sinha, H. Ghosh, M. N. Singh, P. Rajput, C. L. Prajapat, M. R. Singh and G. Ravikumar, *Journal of Applied Physics*, 2014, **116**, 074904-074901-074904-074909.
20. H. Singh, H. Ghosh, T. V. Chandrasekhar Rao, G. Sharma, J. Saha and S. Patnaik, *J. Appl. Phys.*, 2016, **119**, 044104.
21. M. Weil, *Acta Crystallog. Sec. E*, 2006, **62**, i246-i247.
22. J. W. Kim, S. Artyukhin, E. D. Mun, M. Jaime, N. Harrison, A. Hansen, J. J. Yang, Y. S. Oh, D. Vanderbilt, V. S. Zapf and S. W. Cheong, *Phys. Rev. Lett.*, 2015, **115**, 137201.
23. X. Zhu, Z. Wang, X. Su and P. M. Vilarinho, *ACS Appl. Mater. Inter.*, 2014, **6**, 11326-11332.
24. M. Weil, *Acta Crystallog. Sec. E*, 2006, **62**, i244-i245.
25. E. Solana-Madruga, A. J. Dos santos-Garcia, A. M. Arevalo-Lopez, D. Avila-Brande, C. Ritter, J. P. Attfield and R. Saez-Puche, *Dalton Trans.*, 2015, **44**, 20441-20448.
26. G. V. Bazuev, A. P. Tyutyunnik, M. V. Kuznetsov and Y. G. Zainulin, *J. Supercond. Nov. Magn.*, 2018, **31**, 2907-2914.
27. A. J. Dos santos-Garcia, E. Solana-Madruga, C. Ritter, D. Avila-Brande, O. Fabelo and R. Saez-Puche, *Dalton Trans.*, 2015, **44**, 10665-10672.
28. A. M. Arevalo-Lopez, F. Stegemann and J. P. Attfield, *Chem. Commun.*, 2016, **52**, 5558-5560.
29. M.-R. Li, J. P. Hodges, M. Retuerto, Z. Deng, P. W. Stephens, M. C. Croft, X. Deng, G. Kotliar, J. Sánchez-Benítez, D. Walker and M. Greenblatt, *Chem. Mater.*, 2016, **28**, 3148-3158.
30. A. J. D. Santos-García, C. Ritter, E. Solana-Madruga and R. Sáez-Puche, *J. Phy.: Condens. Matter*, 2013, **25**, 206004.
31. R. Mathieu, S. A. Ivanov, I. V. Solovyev, G. V. Bazuev, P. Anil Kumar, P. Lazor and P. Nordblad, *Phys. Rev. B*, 2013, **87**, 014408.
32. A. P. Tyutyunnik, G. V. Bazuev, M. V. Kuznetsov and Y. G. Zainulin, *Mater. Res. Bull.*, 2011, **46**, 1247-1251.
33. M.-R. Li, P. W. Stephens, M. Croft, Z. Deng, W. Li, C. Jin, M. Retuerto, J. P. Hodges, C. E. Frank, M. Wu, D. Walker and M. Greenblatt, *Chem. Mater.*, 2018, **30**, 4508-4514.
34. R. Shannon, *Acta Crystallogr. Sect. A*, 1976, **32**, 751-767.
35. G. Liu, J. Gong, L. Kong, R. D. Schaller, Q. Hu, Z. Liu, S. Yan, W. Yang, C. C. Stoumpos, M. G. Kanatzidis, H.-k. Mao and T. Xu, *Proc. Nati. Acad. Sci.*, 2018, **115**, 8076.
36. Z. Gao, Y. Liu, C. Lu, Y. Xia, L. Fang, Y. Ma, Q. He, D. He and S. Yang, *J. Am. Ceram. Soc.*, 2018, **101**, 2571-2577.
37. M. H. Zhao, W. Wang, Y. Han, X. Xu, Z. Sheng, Y. Wang, M. Wu, C. P. Grams, J. Hemberger, D. Walker, M. Greenblatt and M. R. Li, *Inorg Chem*, 2019, **58**, 1599-1606.
38. R. Mathieu, S. A. Ivanov, P. Nordblad and M. Weil, *Eur.Phys. J. B*, 2013, **86**, 1-4.
39. L. Zhao, Z. Hu, C.-Y. Kuo, T.-W. Pi, M.-K. Wu, L. H. Tjeng and A. C. Komarek, *Phys. Status Solidi RRL*, 2015, **9**, 730-734.

Predicted Polymorph Manipulation in Exotic Double Perovskite Oxide

He-Ping Su,[a] Shu-Fang Li,[b,*] Yi-Feng Han,[b] Mei-Xia Wu,[b] Churen Gui,[c] Yanfen Chang,[d] Mark Croft,[e] Steven Ehrlich,[f] Syed Khalid,[f] Umut Adem,[g] Shuai Dong,[c] Young Sun,[d] Feng Huang,[h] Man-Rong Li[b,*]

Graphic Abstract

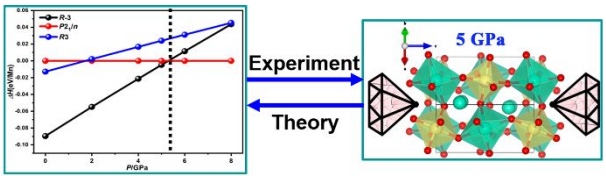

First-principles density functional theory calculations, for the first time, predict the Mg_3TeO_6-to-perovskite type phase transition in Mn_3TeO_6 around 5 GPa.